# Quantitative assessment of laser-induced stress waves generated at confined surfaces*

B. P. Fairand, A. H. Clauer, R. G. Jung, and B. A. Wilcox

*Battelle Columbus Laboratories, Columbus, Ohio 43201*
(Received 22 April 1974; in final form 15 July 1974)

Laser-induced stress waves in iron samples were analyzed by measuring the pressure environment at the back surface of various sample thicknesses. These results were compared with numerical calculations obtained from a one-dimensional radiation hydrodynamics computer code. The experiments were conducted in an air environment under ambient conditions and the metal surfaces were confined by transparent overlays. Peak pressures exceeding 50 kbar were measured with quartz pressure transducers at a laser power density of about $10^9$ W/cm$^2$. Computer predictions agreed favorably with the experimental results and indicated that peak pressures exceeding 100 kbar could be generated by appropriate modifications in the laser environment and target overlay configuration.

Generation of stress waves in solids using high-power pulsed lasers has been pursued for some time.[1-6] Over the past four years various methods to enhance the magnitude of these stress waves by modifications in the target surface conditions have received considerable attention.[7-13] In an earlier study it was established that the in-depth microstructural and mechanical properties of aluminum alloys covered with transparent overlays were significantly altered when they were irradiated in air by a high-power $Q$-switched laser.[14] The laser-induced pressure environment was not monitored in those experiments. However, the high dislocation densities observed from transmission electron micrographs strongly suggested that high-amplitude stress waves, i.e., well above the dynamic yield strength of the material, were being propagated in depth. This paper reports on experiments with iron-base alloys where quartz piezoelectric transducers were used to dynamically measure the pressure environment as a function of sample thickness. The measured shape of the pressure pulse and its magnitude were compared to theoretical calculations performed by a one-dimensional radiation hydrodynamics computer code. Additional computer studies were made to assess the effect of different sample surface configurations on stress wave production. These studies confirmed that peak pressures exceeding 100 kbar can be generated with a high-power $Q$-switched laser.

The experiments were performed with a CGE VD-640 $Q$-switched neodymium glass laser which consists of an oscillator followed by five amplifier stages. This system is capable of emitting up to 500 J of laser energy in a pulse that is approximately triangular in shape with a full width at half-maximum of 20–30 nsec. The laser radiation was focused onto the samples with a 100-cm-focal-length convergent lens. During each of the irradiations the laser energy was measured by splitting off a portion of the laser beam and directing it into a CGE carbon calorimeter. The shape of the laser pulse was monitored with a Hewlett Packard PIN photodiode whose output was fed into a 7904 Tektronix oscilloscope. Shot-to-shot repeatability of the laser pulse shape was very good and a typical trace recorded by the oscilloscope is shown in Fig. 1.

The attenuation of the stress wave was determined by measuring the pressure pulse at the back surface of four different sample thicknesses irradiated with the laser. In all cases the laser-irradiated surface was covered with a 2.5-cm-diam by 0.3-cm-thick disk of fused silica. A pressure measurement for the position near the sample "front surface" was made by sputtering a 0.0014-cm-thick iron film onto a quartz disk. This thickness was selected as being sufficient to avoid excessive heating of the pressure transducer due to transport of thermal energy from the front surface. The remaining samples were of an Fe-3 wt% Si alloy in the form of 1.9-cm-diam disks cut from a rolled plate, then ground and lapped to their final thicknesses. The special attention given to surface finishing of the samples was required to ensure that the quartz transducers were in intimate contact with the back surface of the samples. The overlay-sample-transducer sandwich was held together in a brass holder. The overlay and sample were held firmly against a lapped surface by a fine-threaded brass cap having a 1.65-cm-diam hole for entrance of the laser beam, and the pressure transducer was then threaded up through a center hole in the holder and pulled finger tight against the back surface of the sample. Good coupling between the gauge and sample back

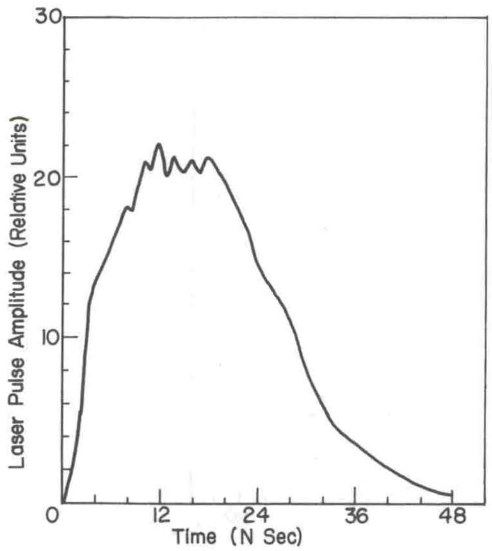


FIG. 1. Laser pulse history.

  

TABLE I. Laser shock-induced peak pressures measured through various thicknesses of iron.

| Sample thickness (cm) | Laser fluence ($J/cm^2$) | Peak pressure (kbar) |
|---|---|---|
| 0.0014 | 31.2 | 56.6 |
| 0.0927 | 31.0 | 18.0 |
| 0.1808 | 28.8 | 8.8 |
| 0.30 | 17.8 | 9.2 |

surface was further ensured by placing a thin layer of mineral oil at this interface.

The peak pressure measured through the various sample thicknesses and the corresponding laser fluences at the sample surface are given in Table I.

The peak pressures presented in Table I were compared to the theoretical predictions of a one-dimensional radiation hydrodynamics computer code which was written to simulate the response of a material during and following the deposition of laser energy. At early times the computer model assumes that the incident radiation is totally absorbed by the solid and the expanding vapor. When the temperature of the expanding vapor is sufficiently high for ionization to be appreciable, absorption of the laser light is governed entirely by a plasma absorption coefficient. The computer model includes an equation of state that takes account of temperature- and density-dependent ionization effects in the plasma phase and blends at low temperatures into a solid-vapor equation of state which contains a sublimation energy model for conversion of the solid into a vapor.[15] The plasma is treated as an ideal gas where the average number of free electrons per ion and ionization energy are determined via simultaneous solution of the Saha equations. The principal energy transport processes

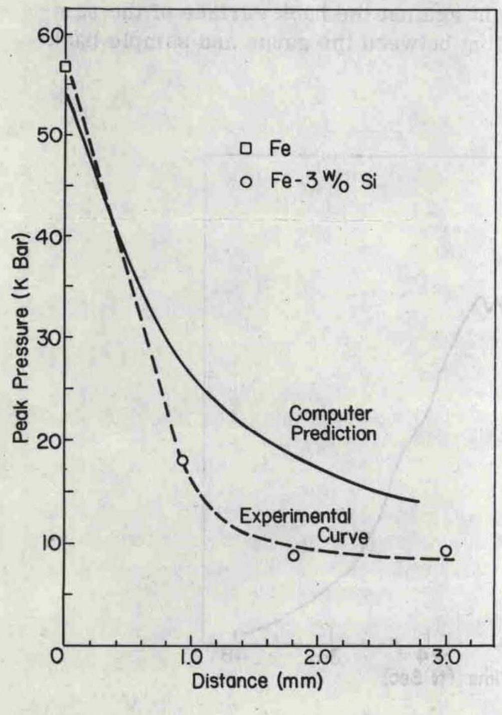


FIG. 2. Peak pressure attenuation in iron-3 wt% silicon.

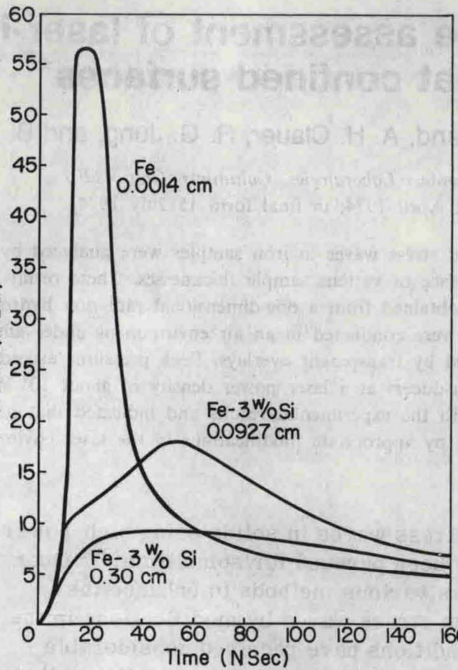


FIG. 3. Stress wave history in iron and iron-3 wt% silicon for various penetration distances.

accounted for in the code are thermal conductivity, which includes conductivity due to ionized electrons,[16] radiation diffusion using a Rosseland mean opacity approximation,[17] and reradiation in the blackbody approximation. Reflection of the incident laser radiation by the plasma is handled in the classical manner wherein the incident laser light is reflected when the plasma frequency exceeds the laser light frequency. The computer model accounts for hydrodynamic attenuation of the stress wave but does not consider material damping mechanisms.

The measured peak pressures presented in Table I are plotted as points joined by the dashed curve in Fig. 2. The solid curve represents the computer prediction for the stress wave attenuation. The laser environment used in this calculation was selected to approximate the experimental conditions, and consisted of a triangular-shaped pulse with a full width at half-maximum of 30 n nsec and a total fluence of 30 $J/cm^2$. As seen from Fig. 2 the computer prediction for the front surface pressure and stress wave attenuation through the first several hundredths of a centimeter of material are in good agreement with the experimental measurements. Deviation of the computer prediction from the experimental curve at deeper penetration can be expected since the model does not account for material, i.e., microstructural damping mechanisms.

The measured shape of the stress wave at different depths into the material provides interesting information on the damping mechanisms and structure of the stress wave. This point is illustrated in Fig. 3, which shows the measured pressure pulse near the sample's front surface and after penetrating through 0.0927 cm and 0.30 cm of iron. The measured pressure profile at 0.0927 cm exhibits a two-component structure, where the faster-moving first wave is an elastic precursor which is followed by the plastic wave. The time difference between the two peaks is consistent with the assumption that the precursor pulse is moving at the elastic dilatational sound velocity and its slower-moving plastic counterpart has a velocity approximately given by the bulk sound speed. Based on the pressure profiles shown in Fig. 3 and the attenuation curves in Fig. 2, it is concluded that the stress wave attenuation through the first 0.05—0.06 cm of material is governed primarily by hydrodynamic effects, and microstructural damping effects become increasingly important thereafter. By the time the wave has passed through 0.3 cm of material it consists almost entirely of an elastic component which is only weakly attenuated as it propagates through additional material. Since the magnitude of this wave is not expected to be a sensitive function of the laser fluence incident on the front surface of the sample, the 0.3-cm-pressure measurement given in Table I and plotted in Fig. 3 was not scaled upward to account for the lower value of laser fluence compared to the other measurements.

Additional computer studies were made in order to investigate the effect of laser fluence, laser energy deposition time, and different overlay configurations on the magnitude and shape of the stress wave generated at the sample's front surface. At the lower laser fluences the code predictions essentially confirmed the results of earlier work by Anderholm[7] who showed that the peak pressure increased approximately as the square root of the laser fluence. However, the code showed this relation did not hold at the higher laser fluences where reflection of light by the blowoff plasma had a dominant effect on both the size and duration of the laser-induced stress wave. Energy loss by reradiation was found to be negligibly small for all of the laser environments studied.

The shape of the stress wave near the sample's front surface was found to be closely related to the time profile of the laser pulse. By lengthening the laser pulse it was possible to lengthen the pressure pulse. The code predicts that pressure pulses several hundred nanoseconds in width can be generated in solids if the appropriate laser environment is incident on its surface.

A final consideration in the computer analysis was an investigation of the effect of placing different thin metal films between the sample surface and transparent overlay. It appeared that the laser-induced peak pressures could be increased by selecting a material with a low heat of vaporization thereby reducing the unproductive use of laser energy to vaporize the material. Lead, which is a readily available metal and has a low heat of vaporization, was initially selected for this study. The presence of the lead overlay did provide about a 20% increase in the peak pressure at a laser fluence of 30 $J/cm^2$. However, at higher fluences the effect of the lead diminished and actually resulted in lower predicted peak pressures than the bare Fe-3 wt% Si surface. This was attributed to the higher degree of ionization present in the lead configuration which both lowered the threshold for the onset of laser light reflection and resulted in a larger fraction of the laser energy being converted into internal energy of the blowoff material. In order to reduce the degree of ionization while preserving the advantageous characteristics of a low sublimation energy material, a zinc overlay was investigated. The results of these calculations were very encouraging and pressures up to 150 kbar were predicted at a laser fluence of 60 $J/cm^2$.

In summary, the experimental results and code predictions confirm our earlier suppositions concerning the magnitude of the laser-induced stress waves. In addition, code calculations demonstrate that significant improvements in both the size and duration of the stress waves can be achieved by appropriate tailoring of the laser environment and sample surface overlay configuration. Experimental studies to confirm these predictions are presently being completed and will be reported at a later date. The particular choice for the iron-base alloy (Fe-3 wt% Si) used in this study was based on the fact that the shock-induced microstructural changes could be quantitatively analyzed by a well-characterized etch-pitting technique.[18] Although the results of this study are still being evaluated, it is evident from examination of the spatial distribution of the stress-wave-induced microstructural changes that radial release waves and stress wave reverberation from sample boundaries play an important role in the final state of the the material's substructure.

*Work sponsored in part by the National Science Foundation.
[1]G.A. Askar'yan and E.M. Moroz, JETP Lett. 16, 1638 (1963).
[2]Frank Neuman, Appl. Phys. Lett. 4, 167 (1964).
[3]David W. Gregg and Scott J. Thomas, J. Appl. Phys. 37, 2787 (1966).
[4]C.H. Skeen and C.M. York, Appl. Phys. Lett. 12, 369 (1968).
[5]Jay A. Fox and Dallas N. Barr, Appl. Phys. Lett. 22, 594 (1973).
[6]J.E. Lowder and L.C. Pettingill, Appl. Phys. Lett. 24, 204 (1974).
[7]N.C. Anderholm, Appl. Phys. Lett. 16, 113 (1970).
[8]L.C. Yang and Vincent J. Menichelli, Appl. Phys. Lett. 19, 473 (1971).
[9]J.D. O'Keefe and C.H. Skeen, Appl. Phys. Lett. 21, 464 (1972).
[10]M. Siegrist and F.K. Kneubuhl, Appl. Phys. 2, 43 (1973).
[11]J.D. O'Keefe and C.H. Skeen, J. Appl. Phys. 44, 4622 (1973).
[12]Jay A. Fox, Appl. Phys. Lett. 24, 461 (1974).
[13]L.C. Yang, J. Appl. Phys. 45, 2601 (1974).
[14]B.P. Fairand, B.A. Wilcox, W.J. Gallagher, and D.N. Williams, J. Appl. Phys. 43, 3893 (1972).
[15]The solid/vapor equation of state and hydordynamics routine are based on the PUFF computer program, Tech Report No. AFWL-TR-66-48, 1966 (unpublished).
[16]Lyman Spitzer, Jr., *Physics of Fully Ionized Gases* (Interscience, New York, 1967), p. 143.
[17]John W. Bond, Jr., Kenneth M. Watson, and Jasper A. Welch, Jr., *Atomic Theory of Gas Dynamics* (Addison-Wesley, Reading, Mass. 1965), p. 371.
[18]G.T. Hahn, P.N. Mincer, and A.R. Rosenfield, Exp. Mech. 11, 248 (1971).